Published in : Journal of the American Society for Mass Spectrometry (2022), vol. 33, pp. 851-858
DOI: 10.1021/jasms.2c00035
Status : Postprint (Author's version)

Cyclic Peptide Protomer Detection in the Gas Phase: Impact on CCS Measurement and Fragmentation Patterns

Andréa McCann[1] (orcid.org/0000-0002-1093-6414), Christopher Kune[1], Philippe Massonnet[1,2] (orcid.org/0000-0002-1326- 692X), Johann Far[1] (orcid.org/ 0000-0003-1208-6262), Marc Ongena[3], Gauthier Eppe[1] (orcid.org/0000-0002-4821-3115), Loïc Quinton[1] (orcid.org/0000-0001-8153-9590), and Edwin De Pauw[1,*] (orcid.org/0000-0003-3475-1315) [1,*]

**Corresponding Author*

[1] *Mass Spectrometry Laboratory, MolSys Research Unit, University of Liege, 4000 Liège, Belgium*

[2] *Maastricht Multimodal Molecular Imaging (M4I) Institute, Division of Imaging Mass Spectrometry, 6229ER Maastricht, Limburg, The Netherlands*

[3] *Gembloux Agro-Bio Tech, University of Liège, 5030 Gembloux, Belgium*

Andréa McCann and Christopher Kune are cofirst authors of this paper.

KEYWORDS: cyclic *lipopeptides, structures, protomers, ion mobility, breakdown curves*

ABSTRACT

With the recent improvements in ion mobility resolution, it is now possible to separate small protomeric tautomers, called protomers. In larger molecules above 1000 Da such as peptides, a few studies suggest that protomers do exist as well and may contribute to their gas-phase conformational heterogeneity. In this work, we observed a CCS distribution that can be explained by the presence of protomers of surfactin, a small lipopeptide with no basic site. Following preliminary density functional theoretical calculations, several protonation sites in the gas phase were energetically favorable in positive ionization mode. Experimentally, at least three near-resolved IM peaks were observed in positive ionization mode, while only one was detected in negative ionization mode. These results were in good agreement with the DFT predictions. CID breakdown curve analysis after IM separation showed different inflection points (CE_{50}) suggesting that different intramolecular interactions were implied in the stabilization of the structures of surfactin. The fragment ratio observed after collision-induced fragmentation was also different, suggesting different ring-opening localizations. All these observations support the presence of protomers on the cyclic peptide moieties of the surfactin. These data strongly suggest that protomeric tautomerism can still be observed on molecules above 1000 Da if the IM resolving power is sufficient. It also supports that the proton localization involves a change in the 3D structure that can affect the experimental CCS and the fragmentation channels of such peptides.

Published in : Journal of the American Society for Mass Spectrometry (2022), vol. 33, pp. 851-858
DOI: 10.1021/jasms.2c00035
Status : Postprint (Author's version)

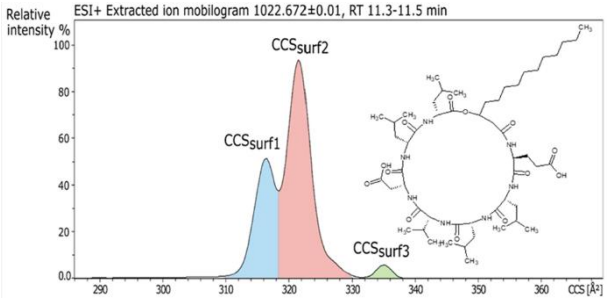

Introduction

Ion mobility (IM) is a technique based on the separation of ions, according to their ion mobility in the gas phase. The ion mobility is related to collision cross section of ions, the nature of the buffer gas (e.g., size or polarizability), and the density number N, based on the Mason-Shamp Equation[1] (eq 1). This equation is valid only under low-field limit conditions, when e/ N is small enough so that K_0 is independent of e/N.[2] When coupled with a mass spectrometer (MS) analyzer, IM adds another dimension of separation, increasing peak capacity and reducing chemical noise.[3,4]

$$K = \frac{3}{16}\frac{e}{N}\left(\frac{2\pi}{\mu k_b T}\right)^{1/2}\frac{z}{\Omega} \quad (1)$$

where *e* is the elementary charge, *N* is the drift gas number density, μ is the reduced mass of the ion-neutral drift gas pair, k_b is the Boltzmann constant, *T* is the temperature, z is the charge of the ion, and Ω is the CCS of the ion. The CCS is a property related to the shape of the ion. Under well-defined conditions, the CCS can be considered as an ion descriptor[5-7] in the same way as its accurate mass. In most IMS methods, the separation takes place in the millisecond time scale[8] allowing the mass and CCS values of each detected ion to be extracted. Ion mobility mass spectrometry (IM-MS) is therefore a powerful structural and analytical technique. Confidence in the CCS values earn interest to improve the analytes' identification accuracy by the MS method, especially for isomeric or near-isomeric compounds.[9-11]

CCS searchable databases are available for many types of small molecules including lipids, steroids, or metabolites.[4,12,13] IM has so far been successfully implemented to conventional LC-MS-based metabolomics and lipidomics workflows and shows promising results in terms of peak capacity, spectral clarity, and fragmentation specificity. Despite a rapidly growing number of available CCS values, the CCS coverage remains however limited due to the lack of available reference standards. The CCS can thus also be calculated based on ab initio computation, but this approach is not a trivial task and is usually reserved to small molecules.[14,15] The last option for CCS extraction is to use a machine-learning algorithm. Several CCS calculations using machine-learning approaches have been already published on lipids[16] and on peptides.[17]

Thanks to high-resolution IM, several published papers have reported the identification of protomeric tautomers,[18-22] also called protomers on small molecules, such as aniline,[23-25] norfloxacin,[26-28] benzocaine,[29] nicotine,[30] or melphalan.[31] Protomeric is an adjective describing a

Published in : Journal of the American Society for Mass Spectrometry (2022), vol. 33, pp. 851-858
DOI: 10.1021/jasms.2c00035
Status : Postprint (Author's version)

particular form of tautomerism, in which the isomers differ only in the proton positions. The protomeric tautomer distribution of an ion is related to its tautomerism energy landscape and the energy provided to this ion. Assuming the population of ions is in microcanonical equilibrium that can be defined by an apparent temperature, a Boltzmann-like distribution can be used to describe the population distribution of the various protomers. The most stable protomers should be the most abundant. However, in IM-MS analysis, protomers are dynamically trapped, and slow isomerization can take place if trapping becomes long enough and if heating occurs during trapping. The prediction of CCS distribution in IM-MS is therefore challenging and will be strongly dependent on the instrument settings (i.e., electrospray source voltage, cone voltage, desolvation temperature, or solvent nature). As an undesired result, one can observe different IMS profiles for the same ion submitted to protomeric tautomerism from one instrument setting to another. The use of a CCS value extracted from an IMS distribution requires then to consider the effect of the protomeric tautomerism, when this can occur.

When it turns to peptide protomers, the presence of a basic residue (lysine, arginine, or histidine) in the peptidic sequence is an energetically favorable site for protonation. The question raised in this work is the following: What are the preferential sites of protonation when there is not a unique favorable site? To answer to this question, we used the lipopeptide surfactin (Figure 1) as a reference compound for protomer exploration, as this molecule does not bear a basic residue in its peptidic sequence. In addition, the surfactin molecule does not form multicharged ions (singly and doubly charged ions are the most common charge states), simplifying the study of protomer formation.

Figure 1. *Surfactin structure.*

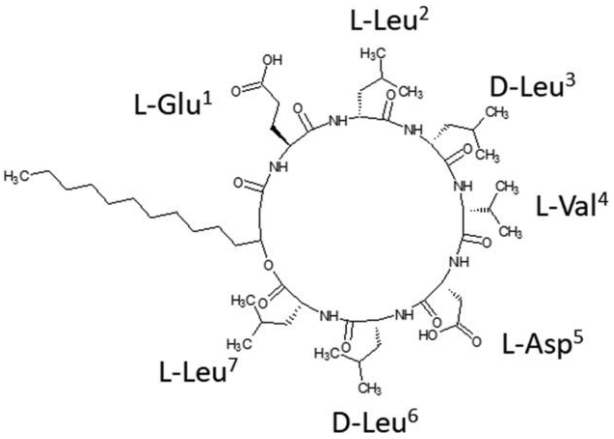

Methods

CHEMICALS. Trifluoroacetic acid (TFA) and formic acid were purchased from Sigma-Aldrich (Overijse, Belgium). Acetonitrile of LC-MS grade was purchased from Biosolve (Valkenswaard, Netherlands).

Published in : Journal of the American Society for Mass Spectrometry (2022), vol. 33, pp. 851-858
DOI: 10.1021/jasms.2c00035
Status : Postprint (Author's version)

SURFACTIN PRODUCTION AND EXTRACTION. The strain used for surfactin production was Bacillus velezensis GA1. The strain was inoculated on a semisolid agar-based PDA (potato dextrose agar) medium and grown for 2 days at 30 °C. Surfactin was extracted by selecting the area of gelified medium corresponding to the Bacillus velezensis GA1 colony and adding 2 mL of 70% ACN. The mixture was vortexed and ultrasonicated for 1 min. After regular stirring for 2 h at room temperature, the extract was evaporated to dryness in a speed-vac instrument and resuspended in 1 mL of pure ACN.

HPLC SEPARATION. Lipopeptides were separated by UPLC (Acquity H-Class, Waters, Milford, MA, USA) on an ACQUITY BEH C18 130 A, 1.7 µm, 1 X 150 mm column (Waters, Milford, MA, USA). The elution was performed at a flow rate of 110 µL/min at 40 °C in 20 min. Mobile phase A corresponds to H_2O with 0.1% formic acid, and mobile phase B corresponds to ACN with 0.1% formic acid. The gradient starts 2 min after the injection at 50% of mobile phase B, reaches 99% after 14 min of the run, and is held for 2 min. Mobile phase B is then lowered to 50% for 4 min for column re-equilibration. The HPLC separation in reverse phase mode of surfactin enables the variants to be eluted according to their lateral chain length and their CH_2 branching mode.

ION MOBILITY MASS SPECTROMETRY. The HPLC-eluted compounds were detected by ion mobility mass spectrometry on a timsTOF instrument (Bruker, Bremen, Germany) in positive and negative ESI mode. The capillary source was set to 3500 V, the nebulizer was set to 4 bar, the dry gas was set to 8.5 L/min, and the dry temperature was set to 200 °C. In ion mobility mode, the TIMS electric field gradient scan time was set to 200 ms with a duty cycle set at 50% unless otherwise specified. The TIMS cell was operated with N_2 as the drift gas. The TIMS ramp start was set to 0.7 and to 0.5 V·s/cm^2 in positive and negative ionization mode, respectively. The TIMS ramp end was set to 2.2 and 1.8 V·s/cm^2 in positive and negative ionization mode, respectively. Quadratic mass calibration and linear ion mobility calibration were performed using Agilent Tune Mix (Agilent Technologies, Santa Clara, CA, USA) from m/z 200 to 2000. For breakdown curve experiments, the ion m/z 1022.6762 ± 0.5 corresponding to singly charged C14 surfactin was selected in the quadrupole and subject to fragmentation by CID with a collision voltage ranging from 5 to 55 V. The breakdown curves were generated by monitoring the signal intensity of the precursor ions upon the collision energy after a signal normalization to the total ion current (TIC). The collisional energy corresponding to a fragmentation of 50% of the precursor ions (CE_{50}) was determined from the inflection point of the breakdown curves after a sigmoid fitting, corresponding to the maximum value of the fitting equation derivative (Gaussian shape).

COMPUTATIONAL CHEMISTRY. All the stable structures of protonated nC14 surfactin were modeled considering all O and N atoms as potential protonation sites. ChemDraw software (ChemOffice 2013 suite, PerkinElmer) was used to design the 2D structure of nC14 surfactin, based on the Norine Database[32] SMILES structure of surfactin. The unprotonated structure was first optimized by molecular mechanics using an MM2 force field with ChemBio3D software.

Finally, stable structures of singly charged surfactin nC14 were obtained from density functional theory (DFT) optimization using Gaussian 09.[33] All atoms were described using the CAM-B3LYP[34]

Published in : Journal of the American Society for Mass Spectrometry (2022), vol. 33, pp. 851-858
DOI: 10.1021/jasms.2c00035
Status : Postprint (Author's version)

functional and the 3-21g basis set. The stable structures were validated with the absence of imaginary values of vibrational frequencies

DATA PROCESSING. The HPLC-IM-MS results were analyzed and extracted with Data Analysis v5.1 (Bruker, Bremen, Germany). Breakdown curves were constructed with an in-house Python software, and graphs were built on JMP (SAS, Cary, NC, USA).

Figure 2. *Extracted ion chromatogram of m/z 1022.6762. The three elution peaks correspond to three different surfactin variants listed in Table 1.*

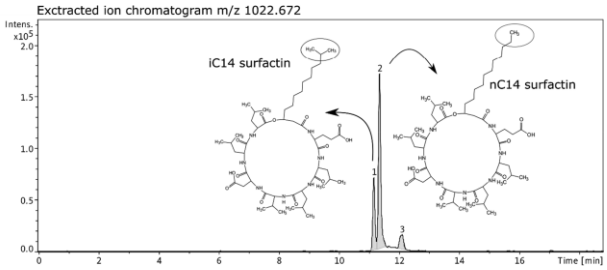

Results and discussion

SCREENING FOR ENERGETICALLY STABLE PROTONATION SITES. In a routine mass-spectrometry-based proteomics experiment, the presence of a C-terminal basic residue (that is often obtained after a trypsin digestion for example) would enhance the ionization in positive mode.[35] In a protomer study, however, the presence of a basic amino acid in every peptide represents a favorable protonation site,[36] and the chances to have several equivalent protonation sites (i.e., leading to protomers) are relatively low. Therefore, the surfactin molecule represents a particularly suitable model for the study of protomers, as there is no basic amino acid in the sequence. A first screen of the number of energetically favorable protonation sites was performed by a computational chemistry approach. All possible protonation sites were taken into account as every heteroatom was considered. For the negative mode, the relative energy of deprotonation sites (corresponding to the acidic residues of asparagine and glutamine) was calculated. The obtained results are provided in the Supporting Information (Figure S2, Table S1).

In positive ionization mode, the calculations show five energetically favorable protonation sites. In the negative ionization mode, only one deprotonation site seems to be energetically favorable. The calculations are compatible with the presence of several protomers of surfactin in the positive ionization mode, while no protomers of surfactin would be detected in the negative ionization mode.

HPLC ISOLATION OF nC14 SURFACTIN. Before the CCS measurement, the different variants of surfactins were previously separated by HPLC, to ensure that the same surfactin structure is considered. The extracted ion chromatogram of m/z 1022.6762 corresponding to singly charged surfactin $(M + H)^+$ shown in Figure 2 presents three elution peaks. Based on the MS/MS results (Figure S1), the two first peaks were identified as C14 surfactin, and the third peak was identified as C15

Published in : Journal of the American Society for Mass Spectrometry (2022), vol. 33, pp. 851-858
DOI: 10.1021/jasms.2c00035
Status : Postprint (Author's version)

surfactin. Since the anteiso configuration is only found in an uneven carbon chain length,[37] the two elution peaks corresponding to surfactin C14 were identified as iso- C14 surfactin (iC14) and linecar-C14 surfactin (nC14), based on the work of Toure et al.[38] The different surfactin variants corresponding to m/z 1022.6762 are listed in Table 1.

Table 1. *m/z 1022.6762 Surfactin Variants*[a]

peak nb	lipopeptides	formula	.retention times (min)	relative proportions
1	surfactin iC14	$C_{52}H_{91}N_7O_{13}$	11.2	25.2
2	surfactin nC14	$C_{52}H_{91}N_7O_{13}$	11.4	66
3	surfactin C15	$C_{52}H_{91}N_7O_{13}$	12.1	8.8

[a]The relative proportions were obtained from the area under the curve

For the following analysis in this work, only the nC14 surfactin variant (corresponding to the second elution compound) will be considered, as it is the variant that is the most present (66% of relative intensity) in the extract.

TRAPPED ION MOBILITY PROFILES OF nC14 SURFACTIN. The ion mobility profile of the RP-HPLC isolated variant of surfactin nC14 was then recorded on the timsTOF instrument in positive and in negative mode ionization. The CCS distribution of m/z 1022.6762 $[M + H]^+$ and m/z 1020.6602 $[M - H]^-$ extracted during the elution of nC14 surfactin (RT 11.4 ± 0.1 min) are displayed in Figure 3. Interestingly, the EIC of nC14 surfactin in positive ionization mode shows three different IM bands (named CCS_{surf1}, CCS_{surf2}, and CCS_{surf3}, corresponding to 316.2, 321.5, and 335.2 A^2, respectively). In negative ionization mode, however, only one IM band is detected at 317.0 A^2. The variants of surfactin being previously separated by RP-HPLC, the IM profile observed corresponds to an identical analyte molecule. The IM profile of nC14 surfactin would therefore suggest the presence of gas-phase charge site isomers (protomers) in positive ionization mode. The proton is suspected to be localized on different atoms and to induce slight changes in the structure that can be observed in ion mobility. In negative ionization mode, however, the ions remain monoisomeric, as only one IM band is observed. These results are in line with the computational calculations results (see Figure S-2, Table S- 1).

The assumption of a prototropism isomerism is reinforced when the accumulation time (before the TIMS elution) is changed while holding the ramp time constant[39,40] (here at 200 ms). As shown in Figure 4 for the protonated nC14 surfactin ions, the ion mobility profile changes when the accumulation time is reduced from 200 to 100 ms (100% to 50% duty cycle, respectively). This suggests that the observed population of nC14 surfactin structures is kinetically trapped in the measurement time scale and changes in function of the accumulation time. A longer accumulation time is expected to allow slower isomerization reaction to occur.

Published in : Journal of the American Society for Mass Spectrometry (2022), vol. 33, pp. 851-858
DOI: 10.1021/jasms.2c00035
Status : Postprint (Author's version)

Figure 3. *EIM of nC14 surfactin in positive (top) and in negative (bottom) mode ionization.*

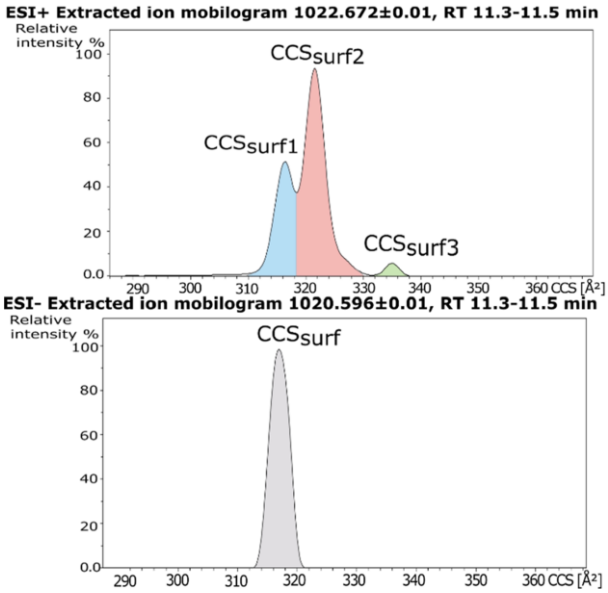

Figure 4. *Extracted ion mobilogram of nC14 surfactin in positive mode ionization. (A) Duty cycle set at 100% (corresponding to 200 ms). (B) Duty cycle set at 50% (corresponding to 100 ms).*

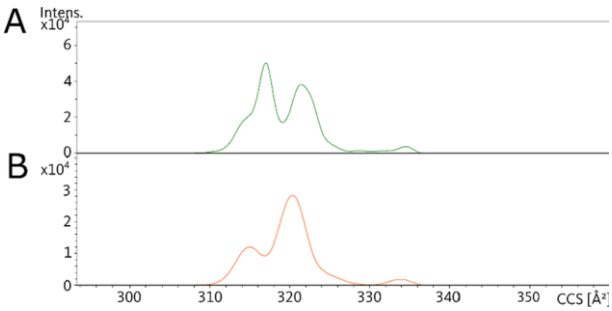

Figure 5. *Survival yield of CCS_{surf1}, CCS_{surf2}, and CCS_{surf3} for collision energies ranging from 5 to 55 eV. The solid lines correspond to the presucrsor ion intensities (normalized to the total ion count). The dashed lines correspond to the fragment ion intensities (normalized to the total ion count).*

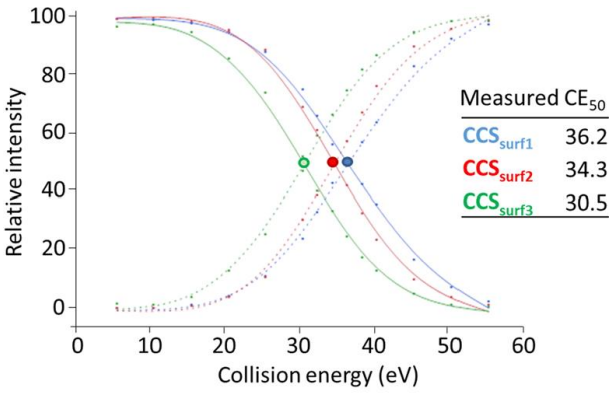

Published in : Journal of the American Society for Mass Spectrometry (2022), vol. 33, pp. 851-858
DOI: 10.1021/jasms.2c00035
Status : Postprint (Author's version)

Figure 6. *(A) LC-IM-MS/MS spectrum of nC14 surfactin, m/z 1022.6762, 40 eV, @RT, 11.4 min, corresponding to the CCS_{surf1} (316.2 $Å^2$). (B) LC-IM-MS/MS spectrum of nC14 surfactin, m/z 1022.6762, 40 eV, @RT, 11.4 min corresponding to the CCS_{surf3} (335.2 $Å^2$). The fragment m/z 794.5632 corresponding to the B_5 fragment (highlighted in yellow) appears to be much more abundant in the MS/MS profile of the CCS_{surf3}. (C,D) Evolutions of the intensities of m/z 794 (red) and m/z 796 (blue) divided by the precursor ion intensity according to the collision energy (eV) for CCS_{surf1} (C) and CCS_{surf3} (D). b^+ ions correspond to a cycle opening at the ester bond, while B^+ fragments correspond to a cycle opening at the peptide bond (between Leu[1] and Leu[2]).*

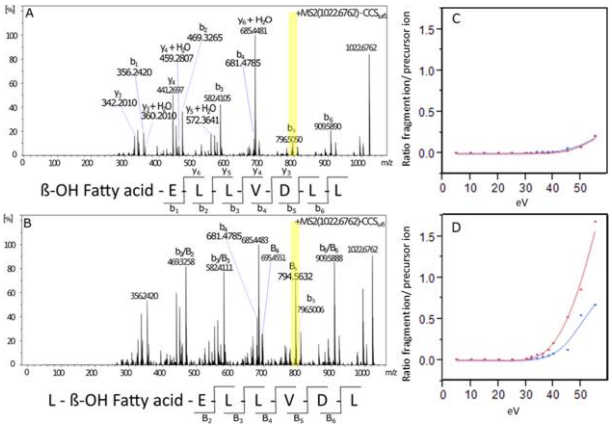

Figure 7. *Suggested fragmentation routes for surfactin ions. (A) Cycle opening occurs at a peptidic bond. Mechanism is adapted from Paizs and Suhai.[45] The obtained B_x fragments are shown in green. (B) Cycle opening occurs at the ester bond, according to the rearrangement mechanism adapted from Yao et al.[46] The obtained b_x fragments are shown in orange. B_3 and b_3 fragments have the same mass (m/z = 582) but not the same structure. Indeed, the B_3 sequence corresponds to L-β-OH fatty acid-E-L, and the b_3 sequence corresponds to β-OH fatty acid-E-L-L.*

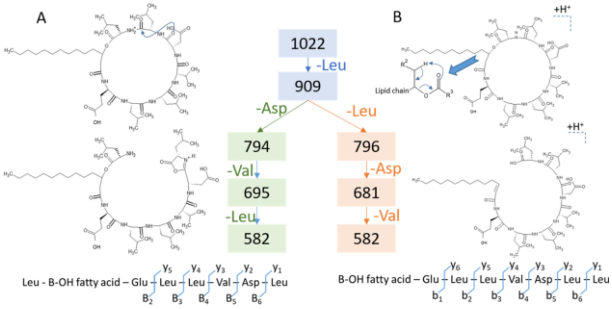

nC14 SURFACTIN SURVIVAL YIELD. The presence of protomers separated by ion mobility mass spectrometry can be further supported by the analysis of fragmentation behavior of the different surfactin ions. The previously separated surfactins CCS_{surf1}, CCS_{surf2}, and CCS_{surf3} were fragmented at different collision energies ranging from 5 to 55 eV. The relative intensity of the precursor ion and the fragments ions are plotted in Figure 5 in function of the collision energy (eV). The survival yields of the three potentially different protomers of surfactins shows different values of CE_{50} for CCS_{surf1}, CCS_{surf2}, and CCS_{surf3} (36.2, 34.3, and 30.5, respectively). If the compounds were identical, the same CE_{50} would have been observed. This result is thus in agreement with the

Published in : Journal of the American Society for Mass Spectrometry (2022), vol. 33, pp. 851-858
DOI: 10.1021/jasms.2c00035
Status : Postprint (Author's version)

protomer hypothesis. Indeed, depending on the proton localization, the different molecules are expected to have different stabilities. The more stable the protomer, the more energy will be required to induce its fragmentation. The CCS_{surf3} appears to be the less stable protomer, as its CE_{50} is the lowest. Oppositely, CCS_{surf1} is the most stable protomer, as its CE_{50} is the highest.

nC14 SURFACTIN FRAGMENTATION. Since surfactin is a cyclic lipopeptide, its fragmentation is expected to take place in a fast two-step process. The peptidic cycle has to first open before fragmentation. The peptidic cycle opening can occur either at a peptidic bond or at the ester bond,[41,42] leading to protonated ring-opened forms with different linear sequences. The protonated ring-opened forms are isobaric and will be immediately fragmented further, as observed through the collision unfolding experiment (CIU) provided in the Supporting Information (Figure S3).

Therefore, the protonated ring-opened forms cannot be detected in IMS. The ring-opening step is thus the surfactin fragmentation. According to the scientific literature, it is commonly reported that the cycle opening occurs at the ester bond.[43,44] Following this initial cleavage, a series of b^+ and y^+ ions can be assigned in the linear sequence β-OH fatty acid- E-L-L-V-D-L-L. These fragments issued from the ester bond cycle opening were detected in the three MS/MS spectra of the surfactins previously separated in ion mobility and are shown in Figure 6A for the CCS_{surf1} ion and in Figure 6B for the CCS_{surf3} ion. For information, MS/MS spectra of CCS_{surf2} are provided in the Supporting Information (Figure S4). This observation confirms that the three surfactin ions separated in ion mobility show the same structure. For example, the fragment $Y_6 + H_2O$atm/z 685.4481, corresponding to the loss of the fatty acyl chain and the glutamine residue, shows that the amino acid chain length remains the same for all the surfactin tautomers separated in ion mobility.

In the MS/MS spectra of the CCS_{surf3} ion shown in Figure 6B, the presence of the fragment m/z 794.5632 is significantly more intense than in the MS/MS spectra of CCS_{surf1} (highlighted in yellow on the figure) and could originate from another cycle opening route. This fragment was identified as part of the serie of B^+ fragments m/z 1022 → 909 → 794 → 695 → 582 → 469, consistent with the loss of Leu, Asp, Val, Leu, and Leu, from the C-terminus. According to these CID fragments, the sequence could be deduced as -β-OH fatty acid-E-L-L-V-D-L, suggesting a ring-opening localization between the amino acids Leu[1] and Leu.[2] The cycle opening mechanism previously described by Paizs and Suhai[45] is shown in Figure 7.

This second fragmentation route is observed in the three surfactin ions separated by IM, but the fragment m/z 794 appears to be up to 6 times more intense for the CCS_{surf3} ions than for the CCS_{surf1} ions (Figure 6C,D). In the CCS_{surf3} ions, the relative intensity of the fragments at m/z 794 (specific to the ring opening between the amino acids Leu[1] and Leu,[2] shown in Figure 7A) is higher than the relative intensity of the fragments at m/z 796 (specific to the ring opening at the ester bond, shown in Figure 7B). It is also worth noticing that both fragment ratios m/z 794 and m/z 796 are more intense in CCS_{surf3} than in CCS_{surf1}, signifying that CCS_{surf3} has a higher fragmentation yield at the same collision energy. These results are in agreement with the obtained survival yield results that suggested that the CCS_{surf3} corresponds to the less stable ions and fragments at lower energy. Finally, in the protomer hypothesis, initial localization of the proton is suspected to modify the surfactin ion stability and to potentially favor another ring-opening site, as it is the case for CCS_{surf3}.

Published in : Journal of the American Society for Mass Spectrometry (2022), vol. 33, pp. 851-858
DOI: 10.1021/jasms.2c00035
Status : Postprint (Author's version)

Conclusion

Our results on surfactin confirm that the presence of protomers is not limited to small molecules and can also occur on peptides, especially when no there is no basic amino acid in the peptide sequence, leaving a distribution of protonation sites. Thanks to computational chemistry, we were able to detect several energetically accessible sites for proton fixation. The presence of protomers of surfactin was confirmed in positive ionization mode by successfully separating the protomers in ion mobility, while no tautomers were observed in the negative ionization mode. Based on this result, a very simple approach to detect protomers can be the comparison of the ion mobility profile of a purified molecule in positive and in negative ionization mode.

The protomer hypothesis was then confirmed with the fragmentation study of surfactins, where another ring-opening localization was detected. So far, the study of protomers in peptides remains at its infancy, but this approach should be beneficial to better understand the fragmentation behavior observed in peptides. The presence of protomers should indeed be taken into account when observing odd fragment intensities, especially when analyzing cyclic peptides.

To conclude, we have shown in this work that for cyclic peptides, the proton can be localized in several energetically equivalent sites, leading to (i) a modification in the structure that can be visible in ion mobility and to (ii) a different ring opening that can be seen in MS/MS analysis.

Associated content

SUPPORTING INFORMATION

The Supporting Information is available free of charge at https://pubs.acs.org/doi/10.1021/jasms.2c00035.

Figures S1-S3 and Table S1 display surfactin fragmentation at different retention times, list of protonation and deprotonation sites with their corresponding localization on the surfactin molecule, surfactin nC14 collision-induced unfolding, and LC-IM-MS/MS spectrum of CCS_{surf2} (PDF)

NOTES

The authors declare no competing financial interest.

ACKNOWLEDGMENTS

A. McCann and C. Kune thank the Excellence Of Science (EOS) Program (Rhizoclip EOS2018000802) of the FNRS F.R.S for financial support. The authors want to thank the TCP group of the University of Liège, especially prof. F. Remacle, for sharing calculation servers allowing the modeling of lipopeptides. Finally, the authors would like to thank D. McCann for his kind review and suggestions.

Published in : Journal of the American Society for Mass Spectrometry (2022), vol. 33, pp. 851-858
DOI: 10.1021/jasms.2c00035
Status : Postprint (Author's version)

References

(1) Mason, E. A.; Schamp, H. W. Mobility of gaseous Ions in weak electric fields. Ann. Phys. 1958, 4 (3), 233-270.

(2) Gabelica, V.; Marklund, E. Fundamentals of ion mobility spectrometry. Curr. Opin. Chem. Biol. 2018, 42, 51-59.

(3) Paglia, G.; Smith, A. J.; Astarita, G. Ion mobility mass spectrometry in the omics era: Challenges and opportunities for metabolomics and lipidomics. Mass Spectrom Rev. 2021. Early view.

(4) May, J. C.; Morris, C. B.; McLean, J. A. Ion Mobility Collision Cross Section Compendium. Anal. Chem. 2017, 89 (2), 1032-1044.

(5) Guntner, A. S.; Thalhamer, B.; Klampfl, C.; Buchberger, W. Collision cross sections obtained with ion mobility mass spectrometry as new descriptor to predict blood-brain barrier permeation by drugs. Sci. Rep. 2019, 9 (1), 19182.

(6) Hernandez-Mesa, M.; Le Bizec, B.; Monteau, F.; Garda- Campana, A. M.; Dervilly-Pinel, G. Collision Cross Section (CCS) Database: An Additional Measure to Characterize Steroids. Anal. Chem. 2018, 90 (7), 4616-4625.

(7) Nichols, C. M.; Dodds, J. N.; Rose, B. S.; Picache, J. A.; Morris, C. B.; Codreanu, S. G.; May, J. C.; Sherrod, S. D.; McLean, J. A. Untargeted Molecular Discovery in Primary Metabolism: Collision Cross Section as a Molecular Descriptor in Ion Mobility-Mass Spectrometry. Anal. Chem. 2018, 90 (24), 14484-14492.

(8) Ruotolo, B. T.; Gillig, K. J.; Stone, E. G.; Russell, D. H. Peak capacity of ion mobility mass spectrometry: separation of peptides in helium buffer gas. J. Chromatogr. B: Anal. Technol. Biomed. Life Sci. 2002, 782 (1-2), 385-392.

(9) Chouinard, C. D.; Beekman, C. R.; Kemperman, R. H. J.; King, H. M.; Yost, R. A. Ion mobility-mass spectrometry separation of steroid structural isomers and epimers. Int. J. Ion Mobil. Spectrom. 2017, 20 (1), 31-39.

(10) Bowman, A. P.; Abzalimov, R. R.; Shvartsburg, A. A. Broad Separation of Isomeric Lipids by High-Resolution Differential Ion Mobility Spectrometry with Tandem Mass Spectrometry. J. Am. Soc. Mass Spectrom. 2017, 28 (8), 1552-1561.

(11) Massonnet, P.; Haler, J. R.; Upert, G.; Degueldre, M.; Morsa, D.; Smargiasso, N.; Mourier, G.; Gilles, N.; Quinton, L.; De Pauw, E. Ion Mobility-Mass Spectrometry as a Tool for the Structural Characterization of Peptides Bearing Intramolecular Disulfide Bond(s). J. Am. Soc. Mass Spectrom. 2016, 27 (10), 1637-46.

(12) Stephan, S.; Hippler, J.; Kohler, T.; Deeb, A. A.; Schmidt, T. C.; Schmitz, O. J. Contaminant screening of wastewater with HPLC-IM- qTOF-MS and LC+LC-IM-qTOF-MS using a CCS database. Anal. Bioanal. Chem. 2016, 408 (24), 6545-6555.

(13) Tejada-Casado, C.; Hernandez-Mesa, M.; Monteau, F.; Lara, F. J.; Olmo-Iruela, M. d.; Garda-Campana, A. M.; Le Bizec, B.; Dervilly- Pinel, G. Collision cross section (CCS) as a complementary parameter to characterize human and veterinary drugs. Anal. Chim. Acta 2018, 1043, 52-63.

(14) Lavanant, H.; Tognetti, V.; Afonso, C. Traveling Wave Ion Mobility Mass Spectrometry and Ab Initio Calculations of Phosphoric Acid Clusters. J. Am. Soc. Mass Spectrom. 2014, 25 (4), 572-580.

Published in : Journal of the American Society for Mass Spectrometry (2022), vol. 33, pp. 851-858
DOI: 10.1021/jasms.2c00035
Status : Postprint (Author's version)

(15) Reading, E.; Munoz-Muriedas, J.; Roberts, A. D.; Dear, G. J.; Robinson, C. V.; Beaumont, C. Elucidation of Drug Metabolite Structural Isomers Using Molecular Modeling Coupled with Ion Mobility Mass Spectrometry. Anal. Chem. 2016, 88 (4), 2273-2280.

(16) Zhou, Z.; Tu, J.; Xiong, X.; Shen, X.; Zhu, Z.-J. LipidCCS: Prediction of Collision Cross-Section Values for Lipids with High Precision To Support Ion Mobility-Mass Spectrometry-Based Lipidomics. Anal. Chem. 2017, 89 (17), 9559-9566.

(17) Meier, F.; Kohler, N. D.; Brunner, A.-D.; Wanka, J.-M. H.; Voytik, E.; Strauss, M. T.; Theis, F. J.; Mann, M. Deep learning the collisional cross sections of the peptide universe from a million experimental values. Nat. Commun. 2021, 12 (1), 1185.

(18) Skinner, O. S.; Breuker, K.; McLafferty, F. W. Charge site mass spectra: conformation-sensitive components of the electron capture dissociation spectrum of a protein. J. Am. Soc. Mass Spectrom. 2013, 24 (6), 807-810.

(19) Cheung See Kit, M.; Carvalho, V. V.; Vilseck, J. Z.; Webb, I. K. Gas-phase ion/ion chemistry for structurally sensitive probes of gaseous protein ion structure: Electrostatic and electrostatic to covalent cross-linking. Int. J. Mass Spectrom. 2021, 463, 116549.

(20) Garabedian, A.; Bolufer, A.; Leng, F.; Fernandez-Lima, F. Peptide Sequence Influence on the Conformational Dynamics and DNA binding of the Intrinsically Disordered AT-Hook 3 Peptide. Sci. Rep. 2018, 8 (1), 10783.

(21) Jeanne Dit Fouque, K.; Kaplan, D.; Voinov, V. G.; Holck, F. H. V.; Jensen, O. N.; Fernandez-Lima, F. Proteoform Differentiation using Tandem Trapped Ion Mobility, Electron Capture Dissociation, and ToF Mass Spectrometry. Anal. Chem. 2021, 93 (27), 9575-9582.

(22) Jeanne Dit Fouque, K.; Wellmann, M.; Leyva Bombuse, D.; Santos-Fernandez, M.; Cintron-Diaz, Y. L.; Gomez-Hernandez, M. E.; Kaplan, D.; Voinov, V. G.; Fernandez-Lima, F. Effective discrimination of gas-phase peptide conformers using TIMS-ECD-ToF MS/ MS. Anal. Meth. 2021, 13 (43), 5216-5223.

(23) Attygalle, A. B.; Xia, H.; Pavlov, J. Influence of Ionization Source Conditions on the Gas-Phase Protomer Distribution of Anilinium and Related Cations. J. Am. Soc. Mass Spectrom. 2017, 28 (8), 1575-1586.

(24) Kune, C.; Delvaux, C.; Haler, J. R. N.; Quinton, L.; Eppe, G.; De Pauw, E.; Far, J. A Mechanistic Study of Protonated Aniline to Protonated Phenol Substitution Considering Tautomerization by Ion Mobility Mass Spectrometry and Tandem Mass Spectrometry. J. Am. Soc. Mass Spectrom. 2019, 30 (11), 2238-2249.

(25) Lalli, P. M.; Iglesias, B. A.; Toma, H. E.; de Sa, G. F.; Daroda, R. J.; Silva Filho, J. C.; Szulejko, J. E.; Araki, K.; Eberlin, M. N. Protomers: formation, separation and characterization via travelling wave ion mobility mass spectrometry. J. Mass Spectrom. 2012, 47 (6), 712-719.

(26) Kaufmann, A.; Butcher, P.; Maden, K.; Widmer, M.; Giles, K.; Uría, D. Are liquid chromatography/electrospray tandem quadrupole fragmentation ratios unequivocal confirmation criteria? Rapid Commun. Mass Spectrom. 2009, 23 (7), 985-98.

(27) Lapthorn, C.; Dines, T. J.; Chowdhry, B. Z.; Perkins, G. L.; Pullen, F. S. Can ion mobility mass spectrometry and density functional theory help elucidate protonation sites in 'small' molecules? Rapid Commun. Mass Spectrom. 2013, 27 (21), 2399-2410.

Published in : Journal of the American Society for Mass Spectrometry (2022), vol. 33, pp. 851-858
DOI: 10.1021/jasms.2c00035
Status : Postprint (Author's version)

(28) McCullagh, M.; Giles, K.; Richardson, K.; Stead, S.; Palmer, M. Investigations into the performance of travelling wave enabled conventional and cyclic ion mobility systems to characterise protomers of fluoroquinolone antibiotic residues. Rapid Commun. Mass Spectrom. 2019, 33 (S2), 11-21.

(29) Warnke, S.; Seo, J.; Boschmans, J.; Sobott, F.; Scrivens, J. H.; Bleiholder, C.; Bowers, M. T.; Gewinner, S.; Schollkopf, W.; Pagel, K.; von Helden, G. Protomers of Benzocaine: Solvent and Permittivity Dependence. J. Am. Chem. Soc. 2015, 137 (12), 4236-4242.

(30) Marlton, S. J. P.; McKinnon, B. I.; Ucur, B.; Maccarone, A. T.; Donald, W. A.; Blanksby, S. J.; Trevitt, A. J. Selecting and identifying gas-phase protonation isomers of nicotineH+ using combined laser, ion mobility and mass spectrometry techniques. Faraday Discuss. 2019, 217 (0), 453-475.

(31) Boschmans, J.; Jacobs, S.; Williams, J. P.; Palmer, M.; Richardson, K.; Giles, K.; Lapthorn, C.; Herrebout, W. A.; Lemière, F.; Sobott, F. Combining density functional theory (DFT) and collision cross-section (CCS) calculations to analyze the gas-phase behaviour of small molecules and their protonation site isomers. Analyst 2016, 141 (13), 4044-4054.

(32) Flissi, A.; Ricart, E.; Campart, C.; Chevalier, M.; Dufresne, Y.; Michalik, J.; Jacques, P.; Flahaut, C.; Lisacek, F.; Leclère, V.; Pupin, M. Norine: update of the nonribosomal peptide resource. Nucleic Acids Res. 2020, 48 (D1), D465-D469.

(33) Frisch, M. J.; Trucks, G. W.; Schlegel, H. B.; Scuseria, G. E.; Robb, M. A.; Cheeseman, J. R.; Scalmani, G.; Barone, V.; Mennucci, B.; Petersson, G. A.; Nakatsuji, H.; Caricato, M.; Li, X.; Hratchian, H. P.; Izmaylov, A. F.; Bloino, J.; Zheng, G.; Sonnenberg, J. L.; Hada, M.; Ehara, M.; Toyota, K.; Fukuda, R.; Hasegawa, J.; Ishida, M.; Nakajima, T.; Honda, Y.; Kitao, O.; Nakai, H.; Vreven, T.; Montgomery, J. A., Jr.; Peralta, J. E.; Ogliaro, F.; Bearpark, M.; Heyd, J. J.; Brothers, E.; Kudin, K. N.; Staroverov, V. N.; Kobayashi, R.; Normand, J.; Raghavachari, K.; Rendell, A.; Burant, J. C.; Iyengar, S. S.; Tomasi, J.; Cossi, M.; Rega, N.; Millam, J. M.; Klene, M.; Knox, J. E.; Cross, J. B.; Bakken, V.; Adamo, C.; Jaramillo, J.; Gomperts, R.; Stratmann, R. E.; Yazyev, O.; Austin, A. J.; Cammi, R.; Pomelli, C.; Ochterski, J. W.; Martin, R. L.; Morokuma, K.; Zakrzewski, V. G.; Voth, G. A.; Salvador, P.; Dannenberg, J. J.; Dapprich, S.; Daniels, A. D.; Farkas, O.; Foresman, J. B.; Ortiz, J. V.; Cioslowski, J.; Fox, D. J. Gaussian 09, revision D.01; Gaussian, Inc.: Wallingford, CT, 2009.

(34) Yanai, T.; Tew, D. P.; Handy, N. C. A new hybrid exchangecorrelation functional using the Coulomb-attenuating method (CAM- B3LYP). Chem. Phys. Lett. 2004, 393 (1), 51-57.

(35) Vandermarliere, E.; Mueller, M.; Martens, L. Getting intimate with trypsin, the leading protease in proteomics. Mass Spectrom Rev. 2013, 32 (6), 453-65.

(36) Wysocki, V. H.; Tsaprailis, G.; Smith, L. L.; Breci, L. A. Mobile and localized protons: a framework for understanding peptide dissociation. J. Mass Spectrom. 2000, 35 (12), 1399-1406.

(37) Theatre, A.; Cano-Prieto, C.; Bartolini, M.; Laurin, Y.; Deleu, M.; Niehren, J.; Fida, T.; Gerbinet, S.; Alanjary, M.; Medema, M. H.; Leonard, A.; Lins, L.; Arabolaza, A.; Gramajo, H.; Gross, H.; Jacques, P. The Surfactin-Like Lipopeptides From Bacillus spp.: Natural Biodiversity and Synthetic Biology for a Broader Application Range. Front. Bioeng. Biotechnol. 2021, 9 (118), 623701.

(38) Toure, Y.; Ongena, M.; Jacques, P.; Guiro, A.; Thonart, P. Role of lipopeptides produced by Bacillus subtilis GA1 in the reduction of grey mould disease caused by Botrytis cinerea on apple. J. Appl. Microbiol. 2004, 96 (5), 1151-1160.

(39) Fernandez-Lima, F.; Kaplan, D. A.; Suetering, J.; Park, M. A. Gas-phase separation using a trapped ion mobility spectrometer. Int. J. Ion Mobil. Spectrom. 2011, 14 (2), 93-98.

Published in : Journal of the American Society for Mass Spectrometry (2022), vol. 33, pp. 851-858
DOI: 10.1021/jasms.2c00035
Status : Postprint (Author's version)

(40) Hernandez, D. R.; Debord, J. D.; Ridgeway, M. E.; Kaplan, D. A.; Park, M. A.; Fernandez-Lima, F. Ion dynamics in a trapped ion mobility spectrometer. Analyst 2014, 139 (8), 1913-1921.

(41) Eckart, K. Mass spectrometry of cyclic peptides. Mass Spectrom Rev. 1994, 13 (1), 23-55.

(42) Hue, N.; Serani, L.; Laprevote, O. Structural investigation of cyclic peptidolipids from Bacillus subtilis by high-energy tandem mass spectrometry. Rapid Commun. Mass Spectrom. 2001, 15 (3), 203-209.

(43) Sabareesh, V.; Ranganayaki, R. S.; Raghothama, S.; Bopanna, M. P.; Balaram, H.; Srinivasan, M. C.; Balaram, P. Identification and Characterization of a Library of Microheterogeneous Cyclohexadep- sipeptides from the Fungus Isaria. J. Nat. Prod. 2007, 70 (5), 715729.

(44) Kecskeméti, A.; Bartal, A.; Bóka, B.; Kredics, L.; Manczinger, L.; Shine, K.; Alharby, N. S.; Khaled, J. M.; Varga, M.; Vágvölgyi, C.; Szekeres, A. High-Frequency Occurrence of Surfactin Monomethyl Isoforms in the Ferment Broth of a Bacillus subtilis Strain Revealed by Ion Trap Mass Spectrometry. Molecules 2018, 23 (9), 2224.

(45) Paizs, B.; Suhai, S. Fragmentation pathways of protonated peptides. Mass Spectrom Rev. 2005, 24 (4), 508-48.

(46) Tang, J.-S.; Zhao, F.; Gao, H.; Dai, Y.; Yao, Z.-H.; Hong, K.; Li, J.; Ye, W.-C.; Yao, X.-S. Characterization and Online Detection of Surfactin Isomers Based on HPLC-MSn Analyses and Their Inhibitory Effects on the Overproduction of Nitric Oxide and the Release of TNF-α and IL-6 in LPS-Induced Macrophages. *Mar. Drugs* 2010, *8* (10), 2605-2618.